2011 IEEE/ASME International Conference on
Advanced Intelligent Mechatronics (AIM2011)
Budapest, Hungary, July 3-7, 2011

Preliminary Experiments on Robotic Assembly using a Hybrid-type Variable Stiffness Actuator

Byeong-Sang Kim, Young-Loul Kim and Jae-Bok Song, *Member, IEEE*

***Abstract*— Precision robotic assembly requires compliant motion to avoid jamming or wedging. To achieve compliant motion, impedance control and a passive compliance device, such as a RCC (remote center compliance) device, have been used in robotic assembly. However, impedance control cannot provide low impedance for the high-frequency range, and load capacity and allowable misalignment of the RCC device are limited. To cope with these problems, we propose to use a variable stiffness actuator in robotic assembly. The 3-DOF manipulator including two HVSAs was developed, and the experiments on robotic assembly were carried out. Two HVSAs provide low impedance to compensate for the lateral and angular errors between the assembly parts. To show the advantages of the HVSA-actuated manipulator over the force-controlled manipulator, we conducted comparison experiments on robotic assembly with the 6-DOF robot manipulator which was controlled by an impedance controller. A series of experiments show that the HVSA-actuated manipulator is more beneficial to execute the tasks requiring both fast motion for high efficiency and low impedance for operational safety.**

I. INTRODUCTION

Commercially available industrial robots generally have the repeatability of 0.05~0.1 mm and the positioning accuracy larger than 0.1 mm without calibration [1]. The positioning error more than 1 mm at the end-effector occurs for an articulated robot manipulator while handling a heavy object due to relatively low stiffness (less than 1 N/μm). In contrary, the clearance between precision elements, such as a bearing, a shaft and a gear etc., is less than 100 μm. When the clearance is small, jamming or wedging can easily occur due to lateral and angular errors. After the assembly parts are jammed, the surface may be scratched by excessive contact force [2]. To deal with this problem, impedance control [3, 4] and passive compliance devices, such as a RCC (remote center compliance) device [5], have been used in robotic assembly.

The implementation of impedance control for a robot manipulator enables low impedance for the low-frequency range, but it is ineffective for the high-frequency range [6]. In other words, the contact motion at high speeds is difficult to achieve when active force control is being implemented. From a practical point of view, however, the speed of the motion or the execution time can in no way be negligible because it is highly related to the cost of the production. On the other hand, a RCC device is beneficial to robotic assembly for small lateral and angular errors. However, load capacity and allowable misalignment are limited [5], and chamfering is required to guide a peg into a hole during assembly.

To cope with these problems, a variable stiffness actuator (VSA), which can simultaneously control the position and stiffness, is used for flexible robotic assembly. A spring installed at the VSA provides low impedance for the high-frequency range, and the output torque can be indirectly controlled by adjusting the deformation of a spring. Therefore, the VSA has all the advantages of active force control and a passive compliance device. In this research, the hybrid type variable stiffness actuator (HVSA) developed in our previous work [8] is used. The HVSA adopts an adjustable moment arm mechanism to have a wide range of stiffness. Similar to other variable stiffness actuators, the HVSA can control the position and stiffness at the same time, and the external torque exerted on the output shaft can be estimated [8-14]. Furthermore, the HVSA can maintain a constant joint stiffness irrespective of the elastic motion of the output shaft. This feature is advantageous to control of the contact force during contact motion.

In this paper, the 3-DOF robot manipulator including two HVSAs is proposed, and the experiments on robotic assembly are carried out. Two HVSAs provide low impedance for the high-frequency range during robotic assembly so as to compensate for the lateral and angular errors between the assembly parts. To show the advantage of the HVSA-actuated manipulator over the force controlled-robot, comparison experiments on robotic assembly are conducted with the 6-DOF robot manipulator which is controlled by the impedance controller. A series of experiments show that the HVSA-actuated manipulator can improve the efficiency of robotic assembly by reducing the assembly time while providing low impedance for operational safety.

The remainder of this paper is organized as follows: the concepts of jamming and wedging are explained in Section II, and the HVSA and its features are briefly presented in Section III. The experimental results on robotic assembly based on the HVSA-actuated manipulator and the force controlled manipulator are shown in Section IV and V, respectively. Finally, Section VI gives our conclusion.

This work was supported by the Center for Autonomous Intelligent Manipulation under the Human Resources Development Program for Convergence Robot Specialists and by the Development of Robotic Systems for High Density Manufacturing funded by the Ministry of Knowledge Economy of Korea.

Byeong-Sang Kim is with the School of Mechanical Eng., Korea University, Seoul, Korea (e-mail: lovidia@korea.ac.kr).

Young-loul Kim is with the School of Mechanical Eng., Korea University, Seoul, Korea (e-mail: kimloul@korea.ac.kr).

Jae-Bok Song (corresponding author) is a Professor of the School of Mechanical Eng., Korea University, Seoul, Korea (Tel.: +82 2 3290 3363; fax: +82 2 3290 3757; e-mail: jbsong@korea.ac.kr))

II. Robotic Assembly

Actual parts have three dimensional shapes, but they can be simplified into two dimensional models when a part has a symmetric shape, as shown in Fig. 1. ε_{l0} and θ_{a0} are the initial lateral and angular errors between a peg and a hole, respectively. The level of difficulty of the assembly depends on these errors.

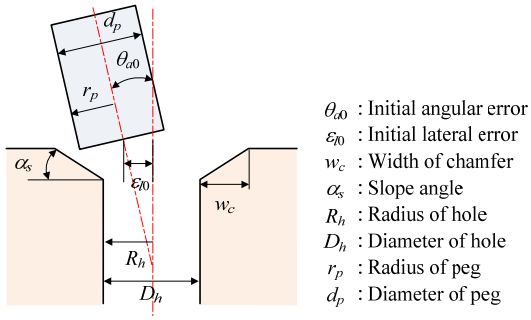

Fig. 1 Two dimensional model of a peg in a hole.

Jamming easily occurs when the insertion force and friction force are misaligned as shown in Fig. 2(a). In this case, the peg can be disassembled by removing the insertion force. On the other hand, if the insertion force is excessively applied with a large misalignment between the peg and the hole, elastic or plastic deformations may occur as shown in Fig. 2(b). In this case, the residual force still remains and thus the peg cannot be disassembled even though the insertion force is removed. This phenomenon is called the wedging, and it is the worst condition during assembly. To avoid jamming and wedging, the magnitude and direction of the insertion force should be controlled, or the position and orientation errors should be compensated to avoid excessive contact force.

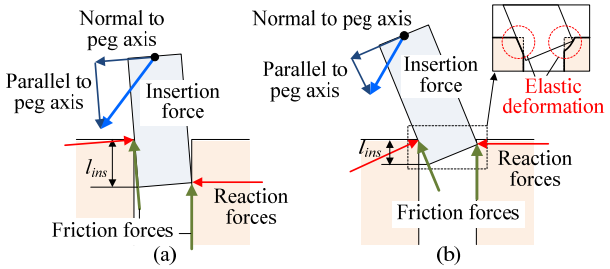

Fig. 2 Jamming and wedging: (a) jamming, and (b) wedging.

III. Hybrid Variable Stiffness Actuator

The hybrid variable stiffness actuator, developed in our previous work, adopted an adjustable moment arm mechanism to provide simultaneous control of position and stiffness. The conceptual model of the adjustable moment arm mechanism is shown in Fig. 3. This mechanism consists of a position frame, an output frame including an output shaft and a lever, and two spring blocks. Both the position and the output frames can rotate around their origin O, and the spring block can move inward or outward along the position frame while supporting the output frame. The rotation angle of the position frame θ_p and the length of the adjustable moment arm r_{sb} are the control parameters associated with the position control and the stiffness control, respectively.

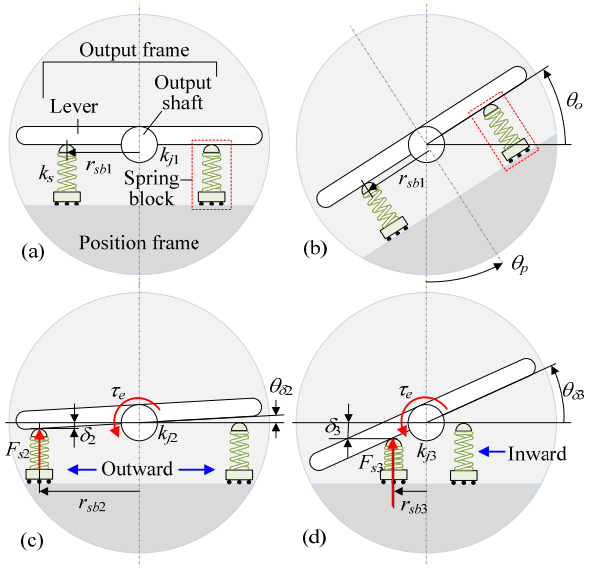

Fig. 3 Concept of variable stiffness actuator based on adjustable moment arm mechanism: (a) initial state, (b) position control, (c) increase in stiffness, and (d) decrease in stiffness.

It is assumed that the initial length of the spring block and the joint stiffness are r_{sb1} and k_{j1}, respectively, and the external torque does not exist (Fig. 3(a)). As shown in Fig. 3(b), the output frame rotates by θ_o as the position frame rotates by θ_p, while maintaining the joint stiffness of k_{j1}. On the other hand, the output frame slightly rotates by $\theta_{\delta 2}$ when the external torque τ_e is exerted on the output frame (Fig. 3(c)), and $\theta_{\delta 2}$ increases to $\theta_{\delta 3}$ as the spring block moves inward (Fig. 3(d)). In other words, the joint stiffness defined by the torque over the rotation angle decreases as the spring block moves inward, and vice versa. Consequently, the simultaneous control of position and stiffness can be achieved by controlling θ_p and r_{sb}.

Figure 4 shows the HVSA based on the adjustable moment arm mechanism, and the details associated with the mechanical structure and its control can be found in Ref. [8]. The total size of the HVSA including two motors is 100 mm (diameter) x 258 mm (length), and the weight of the unit is about 2.36 kg. The maximum continuous torque is 8.5 Nm, the maximum velocity is 450°/s, and the maximum elastic range is ±30°. The range of stiffness variation is 0.07 ~ 2.2 Nm/°, and the response time for stiffness change is 140 ms.

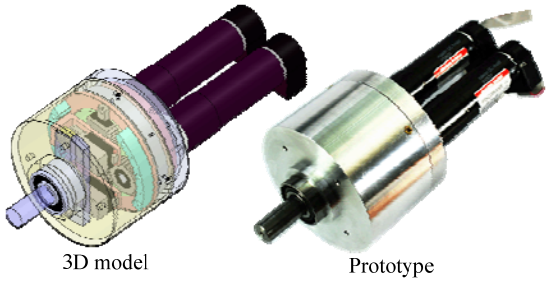

Fig. 4. Hybrid variable stiffness actuator.

IV. Experiments on Robotic Assembly

A. 3-DOF HVSA-Actuated Manipulator

To conduct robotic assembly, the 3-DOF planar manipulator including two HVSAs was constructed, as shown in Fig. 5(a). Two HVSAs were respectively installed at joint 2 and joint 3, and an AC servo motor was connected to joint 1 with a harmonic drive. Figure 5(b) shows the kinematic model of the HVSA-actuated manipulator. The parameter l_i is the length of link i, and θ_i is the joint angle of joint i. From forward kinematics, the position and orientation of the end-effector in Cartesian space can be calculated by

$$\begin{aligned} P_x &= l_1\cos\theta_1 + l_2\cos(\theta_1+\theta_2) + l_3\cos(\theta_1+\theta_2+\theta_3) \\ P_y &= l_1\sin\theta_1 + l_2\sin(\theta_1+\theta_2) + l_3\sin(\theta_1+\theta_2+\theta_3) \\ \theta_e &= \theta_1+\theta_2+\theta_3 \end{aligned} \tag{1}$$

where P_x and P_y are the position of the end-effector in the x and y directions, respectively, and θ_e is the orientation of the end-effector. The length of each link is 8.5 cm, 15 cm, and 22 cm, respectively.

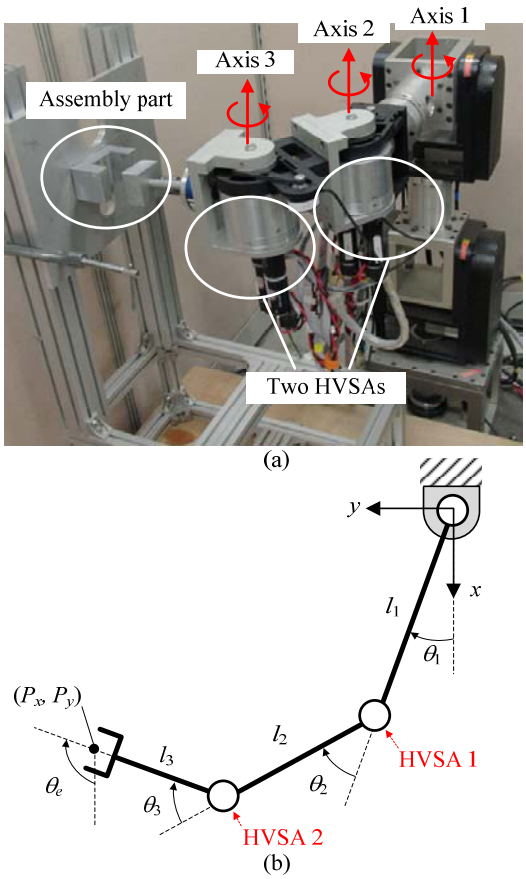

Fig. 5 3-DOF planar manipulator including two HVSAs: (a) constructed manipulator, and (b) kinematic model.

From the partial derivative of (1), the Jacobian matrix is obtained by

$$\begin{aligned} J &= \frac{\partial(P_x, P_y, \theta_e)}{\partial(\theta_1, \theta_2, \theta_3)} \\ &= \begin{bmatrix} -l_1s_1 - l_2s_{12} - l_3s_{123} & -l_2s_{12} - l_3s_{123} & -l_3s_{123} \\ l_1c_1 + l_2c_{12} + l_3c_{123} & l_2c_{12} + l_3c_{123} & l_3c_{123} \\ 1 & 1 & 1 \end{bmatrix} \end{aligned} \tag{2}$$

where $s_1 = \sin(\theta_1)$, $s_{12} = \sin(\theta_1+\theta_2)$, $s_{123} = \sin(\theta_1+\theta_2+\theta_3)$, $c_1 = \cos(\theta_1)$, $c_{12} = \cos(\theta_1+\theta_2)$, and $c_{123} = \cos(\theta_1+\theta_2+\theta_3)$.

The relationship between the joint torque vector τ of a manipulator and the end-effector force vector F can be represented by the following Jacobian relation:

$$\tau = J^T F \tag{3}$$

The differential displacement Δx of the end-effector is related to the differential displacement $\Delta\theta$ of the joint by

$$\Delta x = J \cdot \Delta\theta \tag{4}$$

Substituting (4) together with $\tau = K_j \cdot \Delta\theta$ and $F = K_x \cdot \Delta x$ into (3) yields the relation between the joint stiffness matrix K_j and the Cartesian stiffness matrix K_x as follows:

$$K_j = J^T K_x J \tag{5}$$

From (5), the Cartesian stiffness required for the task can be obtained by adjusting the joint stiffness.

A series of experiments on robotic assembly were carried out using the HVSA-actuated manipulator. The size of the square peg was 50 x 50 x 30 mm, and there was 0.1 mm clearance between the square peg and the square hole. Joint 1 was assumed to be a rigid joint, whereas the stiffness of join 2 and joint 3 were set to 1 Nm/° and 0.5 Nm/°, respectively, to provide compliance. The joint angles for the initial position were set to 0°, 45°, and 45° for joint 1, 2 and 3, respectively. It was also assumed that the lateral and angular errors were less than 1 cm and 3°, respectively.

Figure 6 shows the sequences of robotic assembly. First, the square peg approached the square hole (①). After contact occurred (②), the lateral and angular errors were passively compensated (③) until the assembly was completed (④). Fig. 7 and 8 show the contact force measured by the force/torque sensor in the insertion direction when the assembly speeds were 30 mm/s and 80 mm/s, respectively. The square peg was well inserted into the square hole at both assembly speeds. It took 1.6 s to complete the assembly with the maximum contact force of about -18 N when the assembly speed was 30 mm/s, whereas it took 0.5 s with the maximum contact force of -55 N when the assembly speed was 80 mm/s. The efficiency of robotic assembly was improved by increasing the assembly speed while maintaining low contact force.

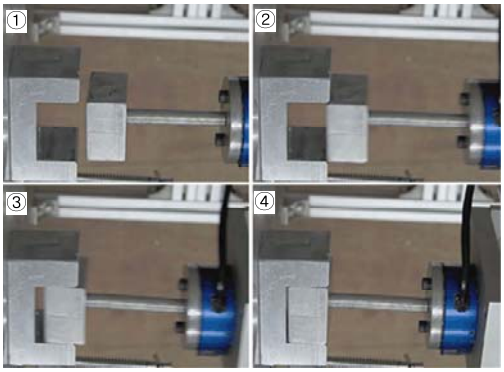

Fig. 6 Sequences of robotic assembly using HVSA-actuated manipulator.

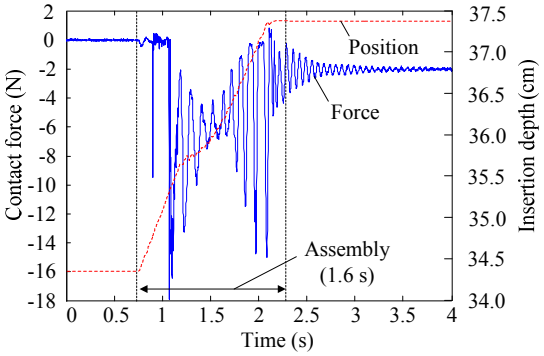

Fig. 7 Experimental results on robotic assembly using HVSA-actuated manipulator (assembly speed: 30 mm/s).

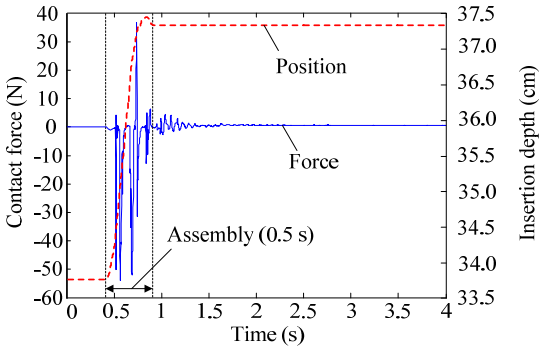

Fig. 8 Experimental result on robotic assembly using HVSA-actuated manipulator (assembly speed: 80 mm/s).

B. 6-DOF Manipulator based on Impedance Control

For comparison experiments, the 6-DOF robot manipulator, which was developed at Korea University, was used, as shown in Fig. 9. Each joint consisting of an AC servo motor and a harmonic drive, which can provide high joint stiffness. The 6-axis force/torque sensor was attached to the wrist to measure the contact force. Impedance control based on a velocity controller was implemented to enable the motion in response to the external force. All motors installed at each joint are controlled at a sampling rate of 1 kHz.

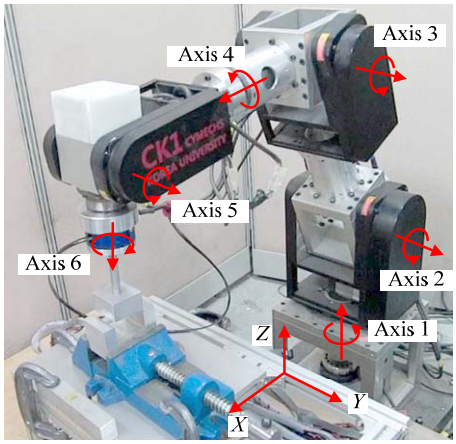

Fig. 9 6-DOF manipulator.

The robotic assembly using a 6-DOF manipulator based on impedance control was conducted, as shown in Fig. 10. Stiffness and damping in Cartesian space were set as follows:

- Translational stiffness: k_x=k_y=500 N/m, k_z=700 N/m
- Rotational stiffness: k_{rx}=k_{ry}=0.5 Nm/^{o}, k_{rz}=0.15 Nm/^{o}
- Translational damping: b_x=b_y= 250 N·s/m, b_z=350 N·s/m
- Rotational damping: b_{rx}=b_{ry}=0.5 Nm·s/^{o}, b_{rz}=0.075 Nm·s/^{o}

These values were empirically determined to provide stable contact motion. During assembly, the robot actively responded to reduce the contact force caused by the misalignment error. Figures 11 and 12 show the contact forces measured by the force/torque sensor when the assembly speeds were 15 mm/s and 30 mm/s, respectively. It took 7 s to complete the assembly with the maximum contact force of about 38 N when the assembly speed was 15 mm/s, whereas it took 4 s with the maximum contact force of 90 N when the assembly speed was 30 mm/s.

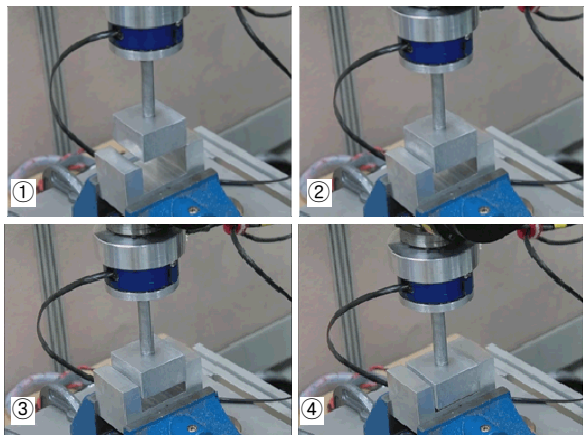

Fig. 10 Sequences of robotic assembly using 6-DOF manipulator.

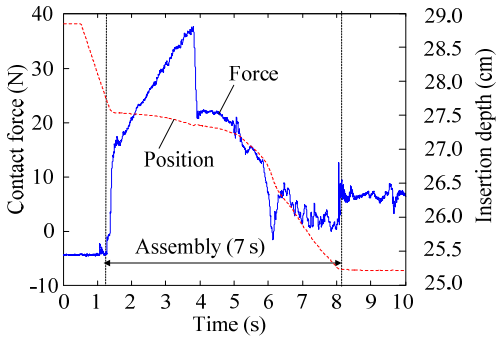

Fig. 11 Experimental results on robotic assembly using 6-DOF manipulator based on impedance control (assembly speed: 15 mm/s)

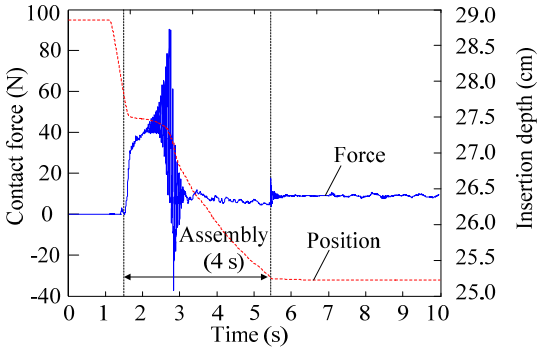

Fig. 12 Experimental results on robotic assembly using 6-DOF manipulator based on impedance control (assembly speed: 30 mm/s).

As shown in the experimental results, the contact force increased with the assembly speed. Compared to the experimental results using the HVSA-actuated manipulator, the higher contact force was generated even though the assembly motion was slow. Reduction in the contact force in the high speed motion requires low impedance for the high-frequency range. However, the manipulator based on active force control has bandwidth limitations in impedance regulation [6, 7], so the fast motion with operational safety is limited.

V. 5 CONCLUSIONS

The robotic assembly based on the variable stiffness actuator (VSA), which can simultaneously control position and stiffness, was proposed to provide flexible robotic assembly. The 3-DOF manipulator including two HVSAs was constructed, and a series of experiments on robotic assembly were conducted. To verify the performance of robotic assembly based on the HVSA-actuated manipulator, the force-controlled robot manipulator was compared. From the comparison experiments, the following conclusions are drawn:

(1) The rigid robot manipulator based on active force control such as impedance control has bandwidth limitation in impedance regulation. Therefore, the task speed is limited to ensure operational safety when the robot executes the tasks requiring contact motion.

(2) The spring installed at the HVSA can provide low impedance for the high-frequency range. Therefore, the HVSA-actuated manipulator can reduce the execution time by increasing the speed of the motion while maintaining operational safety.

REFERENCES

[1] Z. Pan, H. Zhang, Z. Zhu, and J. Wang, "Chatter Analysis of Robotic Machining Process," *Journal of Materials Processing Technology*, vol. 173, pp.301-309, 2006.

[2] D. E. Whitney, "Mechanical Assemblies," *Oxford University Press*, pp.253-292, 2004.

[3] D. P. Gravel, and W. S. Newman, "Flexible Robotic Assembly Efforts at Ford Motor Company," *Proc. of the IEEE International Symposium on Intelligent Control*, pp. 173-182, 2001.

[4] G. D. Glosser, and W. S. Newman, "The Implementation of a Natural Admittance Controller on an Industrial Manipulator," *Proceeding of the IEEE International Conference on Robotics and Automation*, pp. 1209-1215, 1994.

[5] ATI Industrial Automation (http://www.ati-ia.com/products/compliance/Compensator_main.aspx)

[6] D. W. Robinson, "Design and Analysis of Series Elasticity in Closed-loop Actuator Force Control," Ph.D Thesis, Massachusetts Institute of Technology, 2000.

[7] S. D. Eppinger, and W. P. Seering, "Understanding Bandwidth Limitations in Robot Force Control," *Proceedings of the IEEE International Conference on Robotics and Automation*, pp. 904-909, 1987.

[8] B. S. Kim and J. -B. Song, "Hybrid Dual Actuator Unit: A Design of a Variable Stiffness Actuator based on an Adjustable Moment Arm Mechanism," in *Proceeding of the IEEE International Conference on Robotics and Automation*, pp. 1665-1660, 2010.

[9] R. V. Ham, T. G. Sugar, B. Vanderborght, K. W. Lollander and D. Lefeber, "Compliant Actuator Designs," *IEEE Robotics and Automation Magazine*, pp. 81-94, 2009.

[10] G. Tonietti, R. Schiavi, A. Bicchi, "Optimal Mechanical/Control Design for Safe and Fast Robotics," *Experimental Robotics IX: The 9th International Symposium on Experimental Robotics*, vol. 21, pp. 311-320, 2006.

[11] O. Eiberger, S. Haddadin, M. Weis, A. Albu-Schaffer and G. Hirzinger, "On joint Design with Intrinsic Variable Compliance: Derivation of the DLR QA-Joint," in *Proc. of the IEEE International Conference on Robotics and Automation*, pp. 1687-1694, 2010.

[12] A. Albu-Schaffer , S. Wolf, O. Eiberger, S. Haddadin, F. Petit and M. Chalon, "Dynamic Modeling and Control of Variable Stiffness Actuators," in *Proc. of the IEEE International Conference on Robotics and Automation*, pp. 2155-2162, 2010.

[13] B. S. Kim, J. B. Song and J. J. Park, "A Serial-type Dual Actuator Unit with Planetary Gear Train: Basic Design and Applications," *IEEE/ASME Transactions on Mechatronics*, vol. 15, no. 1, 2010.

[14] K. H. Nam, B. S. Kim and J. B. Song, "Compliant Actuation of Parallel-type Variable Stiffness Actuator based on Antagonistic Actuation," *Journal of Mechanical Science and Technology*, , vol. 24, no. 11, pp. 2315-2321, 2010.